# Cisplatin–cyclooxygenase inhibitor conjugates, free and immobilised in mesoporous silica SBA-15, prove highly potent against triple-negative MDA-MB-468 breast cancer cell line

Ivana Predarska[a,b], Mohamad Saoud[c], Ibrahim Morgan[c], Thomas Eichhorn[b], G. N. Kaluđerović[b,c,*] and Evamarie Hey-Hawkins[a,*]

[a] *Universität Leipzig, Faculty of Chemistry and Mineralogy, Institute of Inorganic Chemistry, Johannisallee 29, 04103 Leipzig, Germany.*

[b] *Department of Engineering and Natural Sciences, University of Applied Sciences Merseburg, Eberhard-Leibnitz-Str. 2, 06217 Merseburg, Germany.*

[c] *Department of Bioorganic Chemistry, Leibniz Institute of Plant Biochemistry, Weinberg 3, D 06120 Halle (Saale) Germany.*

## Electronic Supplementary Information

Table of Contents

## Characterisation of conjugates

### Spectra of conjugate **1**

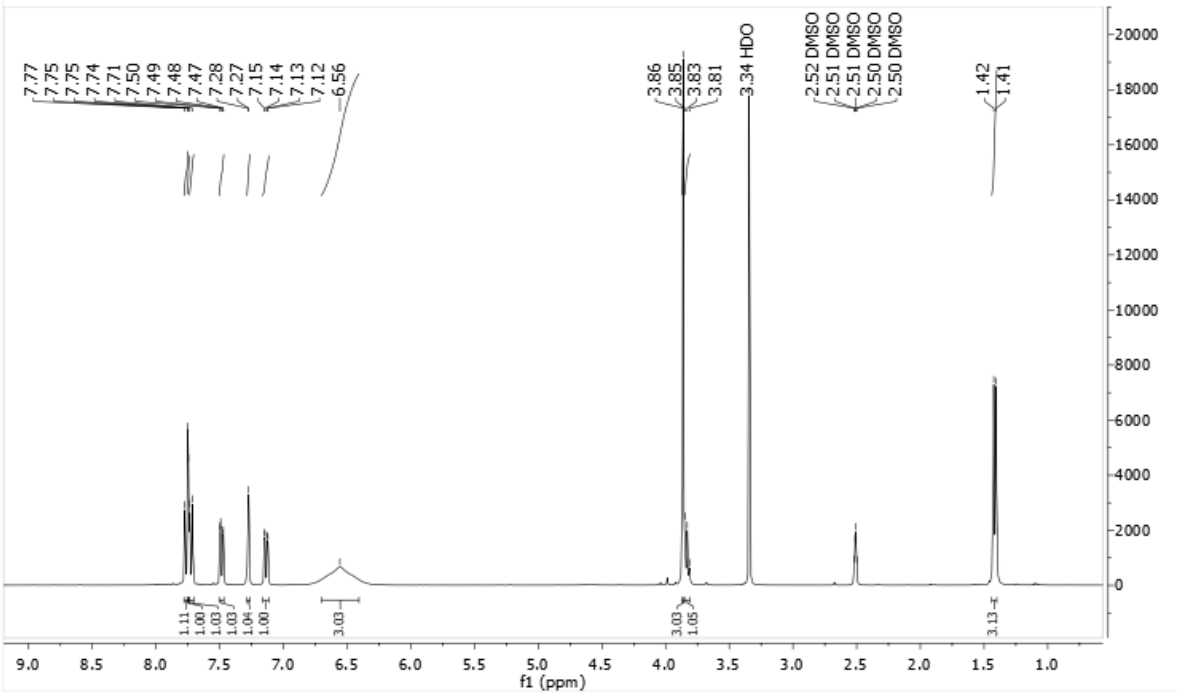


**Figure S1**. $^{1}$H NMR spectrum of **1** in $d_6$-DMSO.

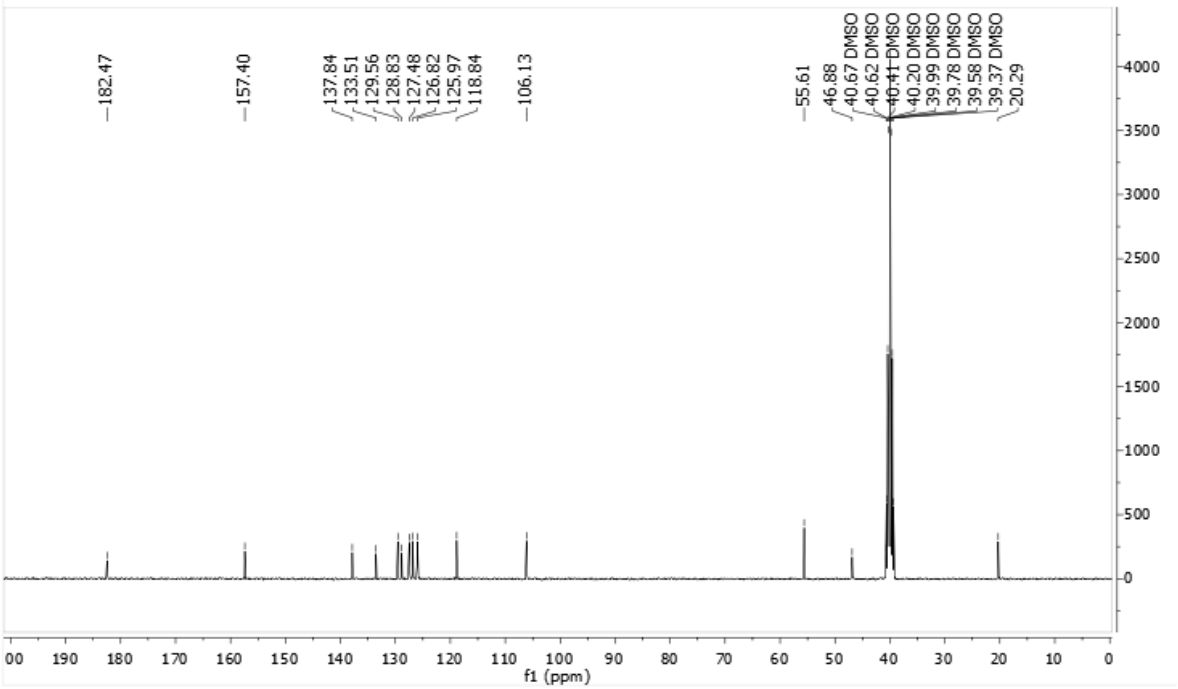


**Figure S2.** $^{13}$C{$^{1}$H} NMR spectrum of **1** in $d_6$-DMSO.

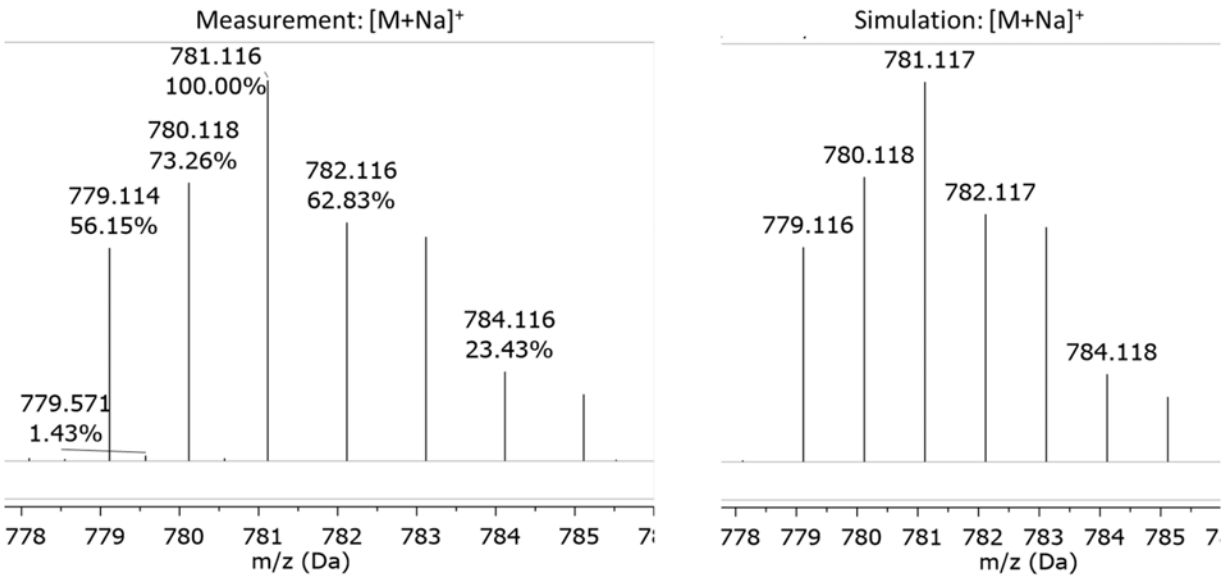


**Figure S3.** HR-ESI-MS (positive mode, $CH_3OH$) of **1**, *m/z* $[M+Na]^+$.

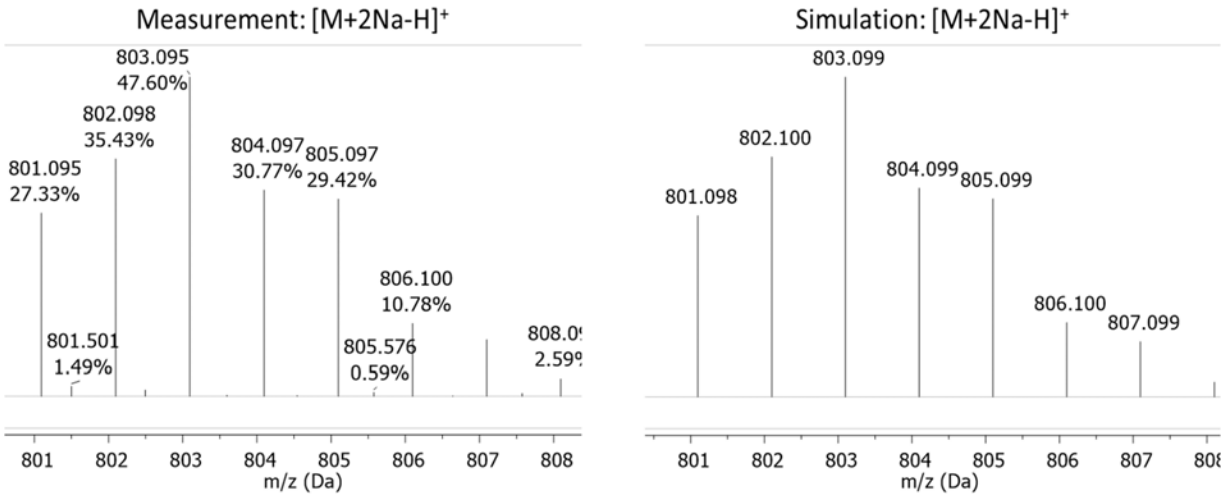


**Figure S4.** HR-ESI-MS (positive mode, $CH_3OH$) of **1**, *m/z* $[M+2Na-H]^+$.

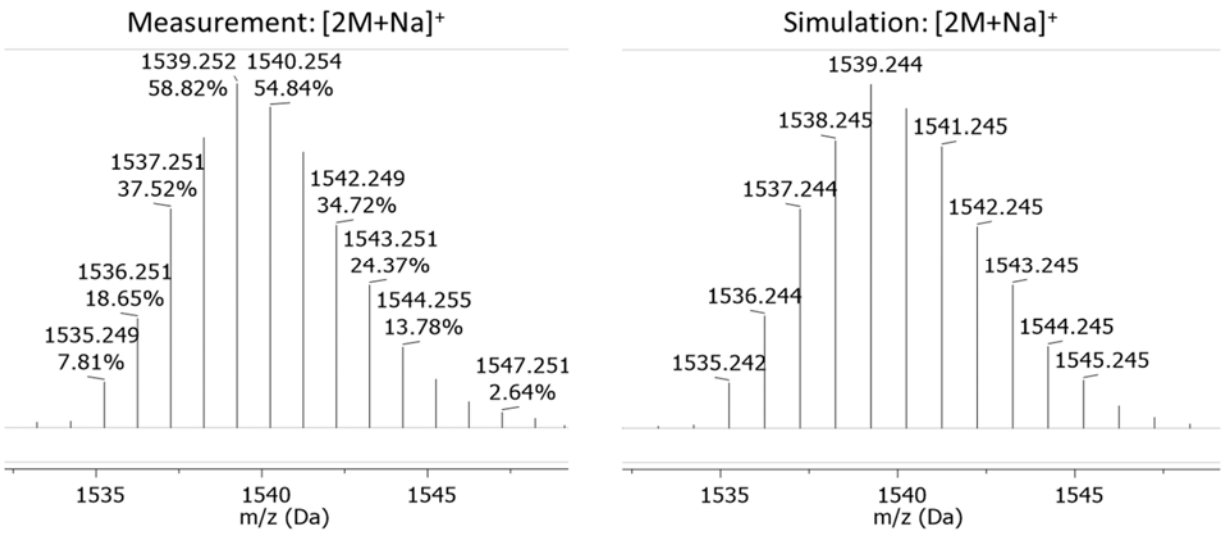


**Figure S5.** HR-ESI-MS (positive mode, $CH_3OH$) of **1**, *m/z* $[2M+Na]^+$.

## Spectra of conjugate **2**

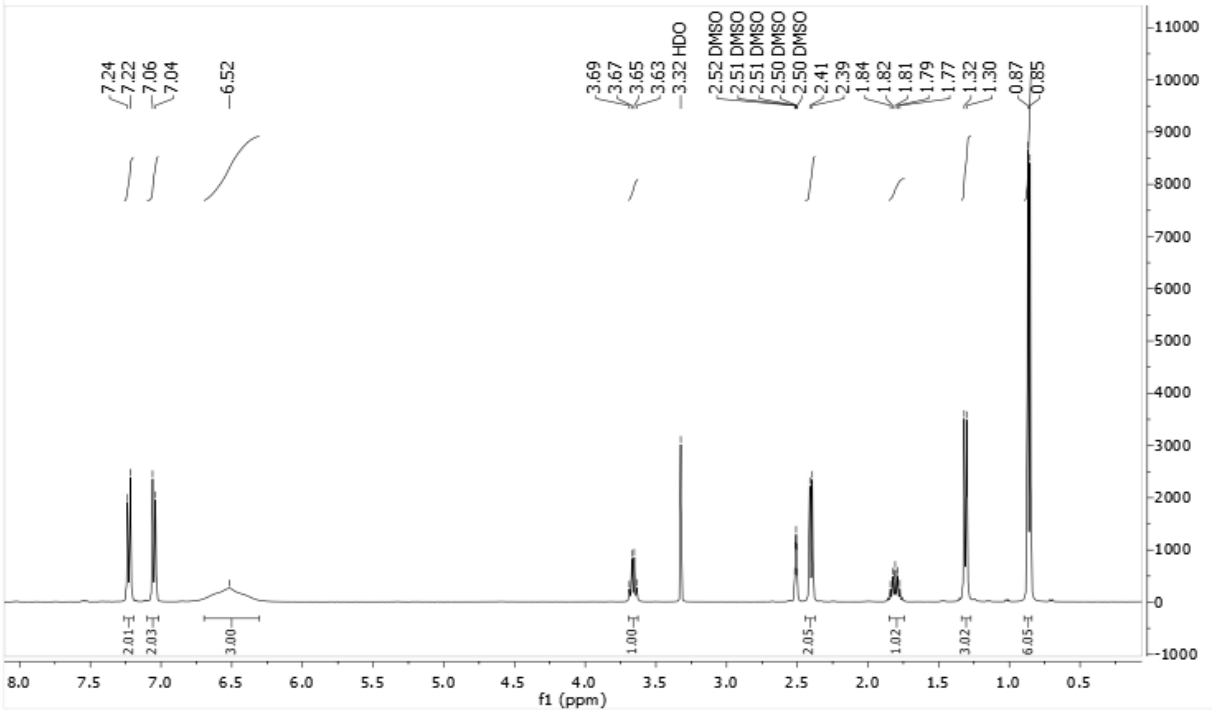


**Figure S6.** $^1H$ NMR spectrum of **2** in $d_6$-DMSO.

**$^1H$ NMR ($d_6$-DMSO, ppm):** $\delta$ = 7.23 (d, $^3J_{HH}$ = 8 Hz, 2H, $CH_{aromat}$), 7.05 (d, $^3J_{HH}$ = 8 Hz, 2H, $CH_{aromat}$), 6.80 – 6.30 (br, 3H, $NH_3$), 3.66 (q, $^3J_{HH}$ = 7 Hz, 1H, CH), 2.40 (d, $^3J_{HH}$ = 7 Hz, 2H, $CH_2$), 1.81 (m, 1H, CH), 1.31 (d, $^3J_{HH}$ = 7 Hz, 3H, $CH_3$), 0.86 (d, $^3J_{HH}$ = 7 Hz, 6H, $CH_3$).

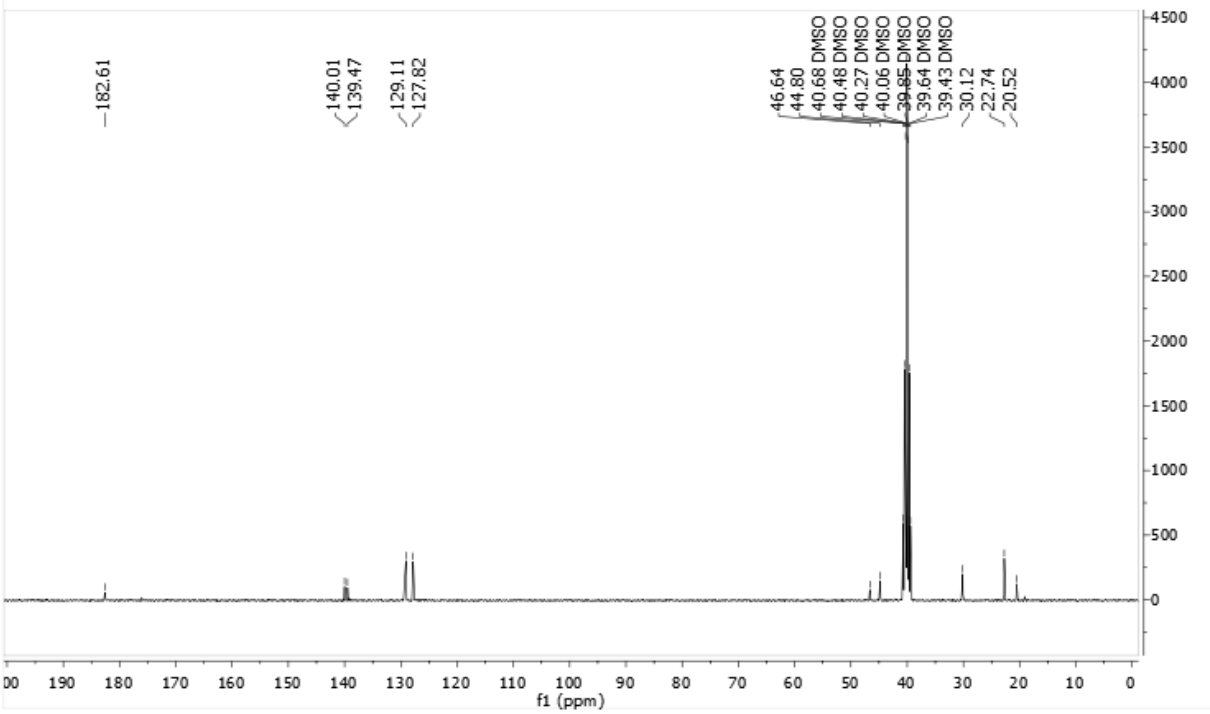


**Figure S7.** $^{13}C\{^{1}H\}$ NMR spectrum of **2** in $d_6$-DMSO.

**$^{13}C\{^{1}H\}$ NMR ($d_6$-DMSO, ppm)**: $\delta$ = 182.6 (qC, COOH), 140.0 (qC, $C_{aromat}$), 139.5 (qC, $C_{aromat}$), 129.1 (2 C, CH, $C_{aromat}$), 127.8 (2 C, CH, $C_{aromat}$), 46.6 (CH, $CHCH_3$), 44.8 ($CH_2$), 30.1 (CH, $CH(CH_3)_2$), 22.7 (2 C, $CH_3$, $CH(CH_3)_2$), 20.5 ($CH_3$, $CHCH_3$).

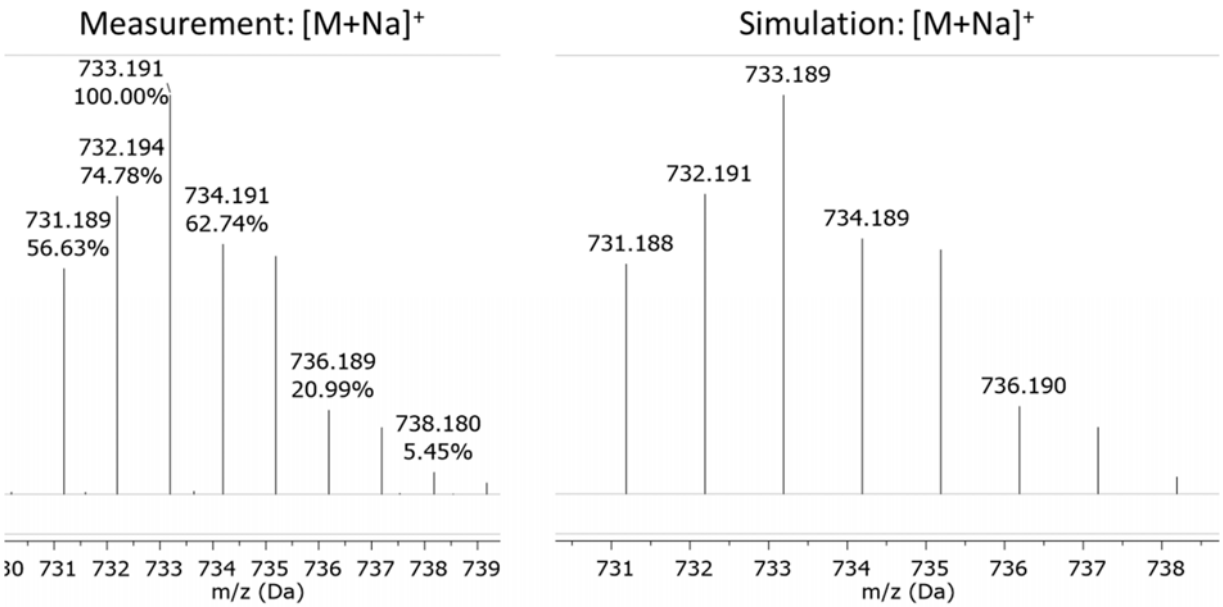


**Figure S8.** HR-ESI-MS (positive mode, $CH_3OH$) of **2**, *m/z* $[M+Na]^+$.

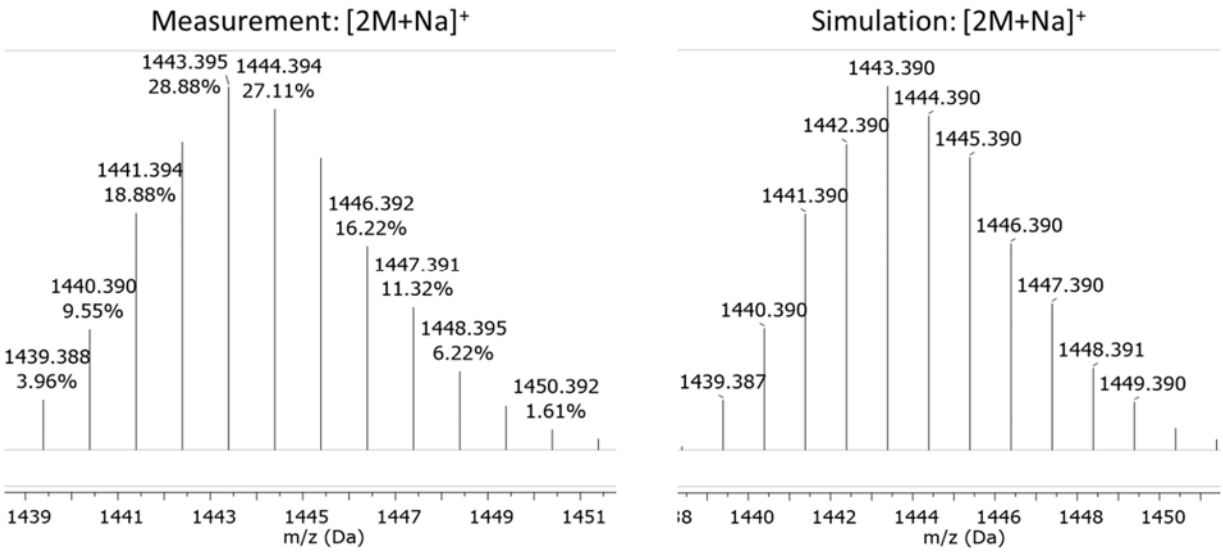


**Figure S9.** HR-ESI-MS (positive mode, $CH_3OH$) of **2**, *m/z* $[2M+Na]^+$.

**HR-ESI-MS (positive mode, $CH_3OH$):** *m/z* $[M+Na]^+$: calcd. for $C_{26}H_{40}Cl_2N_2O_4PtNa$: 733.189, found: 733.191; *m/z* $[2M+Na]^+$: calcd. for $C_{52}H_{80}Cl_4N_4O_8Pt_2Na$: 1443.390, found: 1443.395; the observed isotopic pattern is in agreement with the calculated one.

**Elemental Analysis:** calcd. (%) for $C_{26}H_{40}Cl_2N_2O_4Pt$: C 43.95, H 5.67, N 3.94; found: C 43.60, H 5.22, N 3.72.

## Spectra of conjugate 3

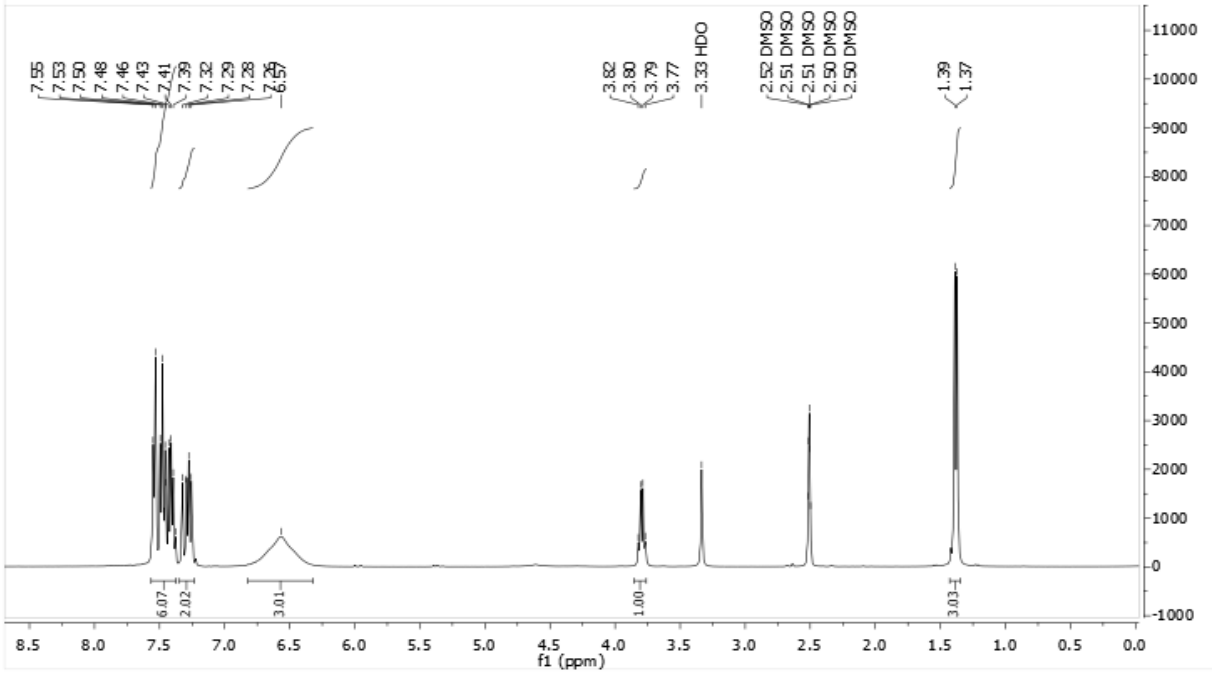


**Figure S10.** $^1H$ NMR spectrum of **3** in $d_6$-DMSO.

**$^1$H NMR ($d_6$-DMSO, ppm):** $\delta$ = 7.55 – 7.38 (m, 6H, $CH_{aromat}$), 7.32 – 7.26 (m, 2H, $CH_{aromat}$), 6.80 – 6.30 (br, 3H, $NH_3$), 3.79 (q, $^3J_{HH}$ = 7 Hz, 1H, CH), 1.38 (d, $^3J_{HH}$ = 7 Hz, 3H, $CH_3$).

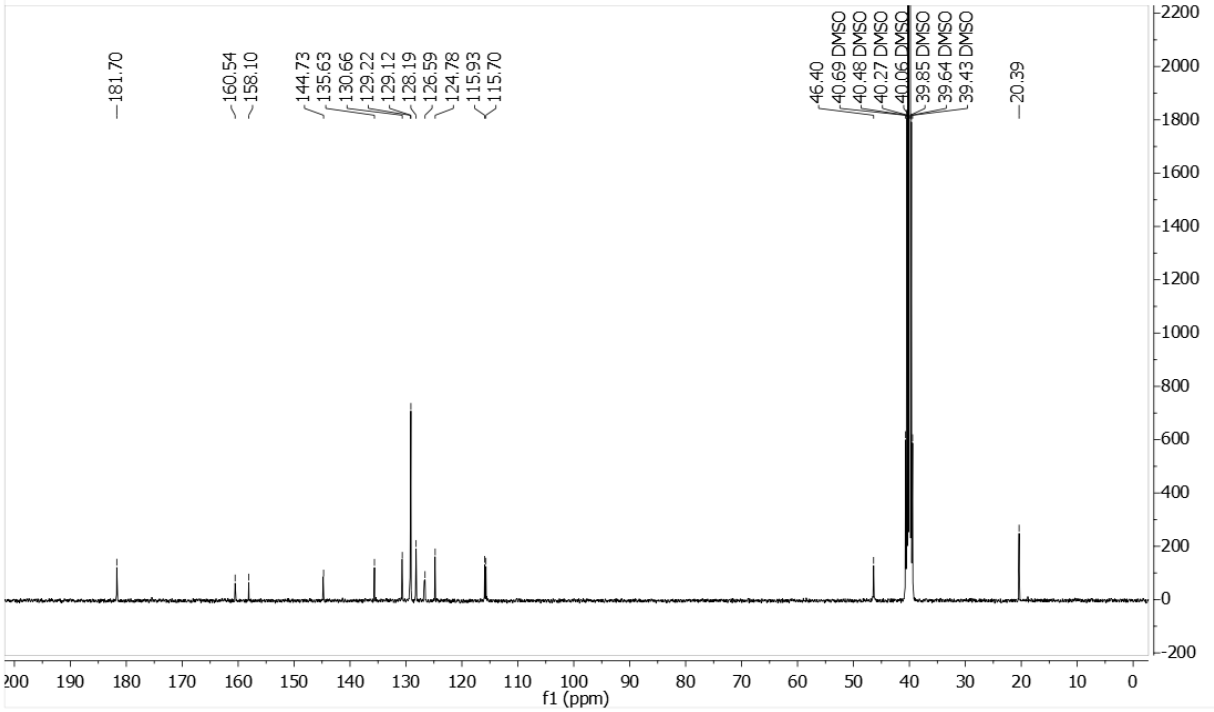


**Figure S11.** $^{13}C\{^1H\}$ NMR spectrum of **3** in $d_6$-DMSO.

**$^{13}C\{^1H\}$ NMR ($d_6$-DMSO, ppm)**: $\delta$ = 181.7 (qC, COOH), 160.5 (qC, $C_{aromat}$), 158.1 (qC, $C_{aromat}$), 144.7 (qC, $C_{aromat}$), 135.6 (qC, $C_{aromat}$), 130.6 (CH, $C_{aromat}$), 129.2 (CH, $C_{aromat}$), 129.1 (CH, $C_{aromat}$), 128.1 (CH, $C_{aromat}$), 126.6 (CH, $C_{aromat}$), 124.7 (CH, $C_{aromat}$), 115.9 (CH, $C_{aromat}$), 115.7 (CH, $C_{aromat}$), 46.4 (CH, $CHCH_3$), 20.4 ($CH_3$, $CHCH_3$).

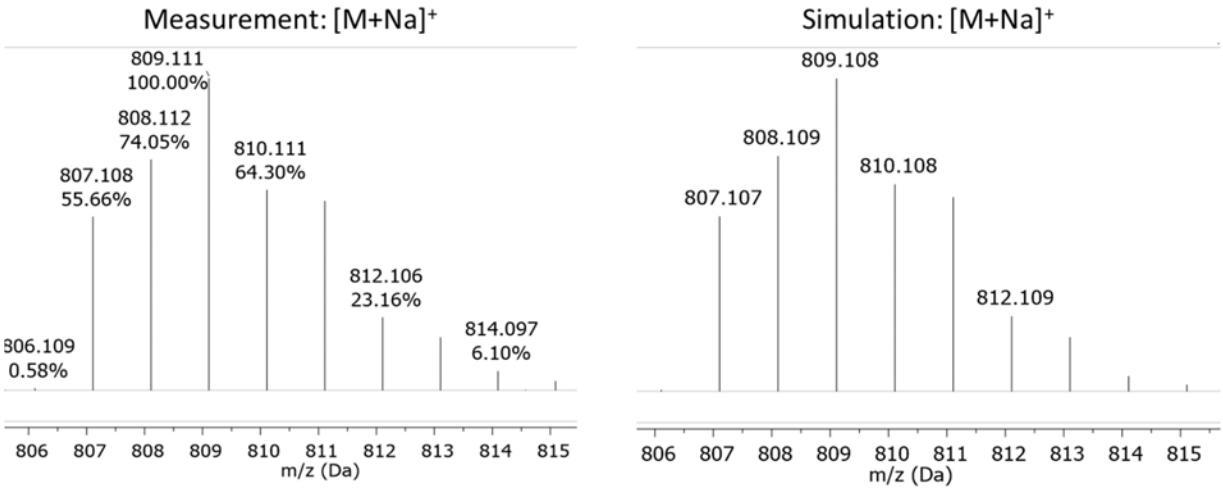


**Figure S12.** HR-ESI-MS (positive mode, $CH_3OH$) of **3**, *m/z* $[M+Na]^+$.

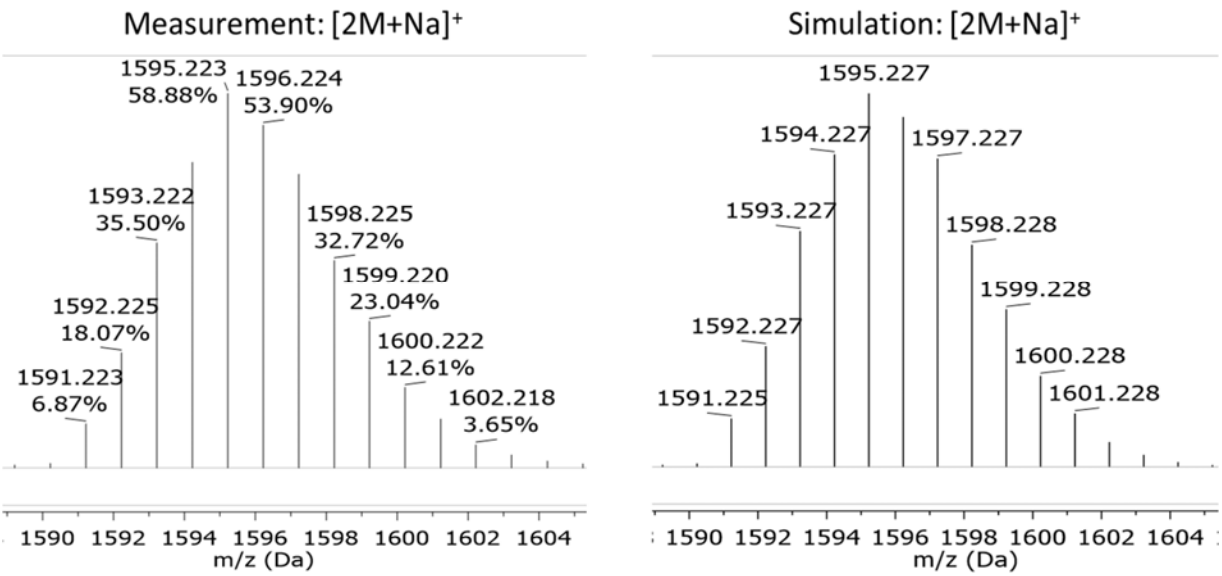


**Figure S13.** HR-ESI-MS (positive mode, $CH_3OH$) of **3**, *m/z* $[2M+Na]^+$.

**HR-ESI-MS (positive mode, DMSO):** *m/z* $[M+Na]^+$: calcd. for $C_{30}H_{30}Cl_2F_2N_2O_4PtNa$: 809.108, found: 809.111; *m/z* $[2M+Na]^+$: calcd. for $C_{60}H_{60}Cl_4F_4N_4O_8Pt_2Na$: 1595.227, found: 1595.223; the observed isotopic pattern is in agreement with the calculated one.

**Elemental Analysis:** calcd. (%) for $C_{30}H_{30}Cl_2F_2N_2O_4Pt$: C 45.81, H 3.84, N 3.56; found: C 45.60, H 3.57, N 3.64.

## Complex stability in DMSO

The stability of conjugate **1** in $d_6$-DMSO solution was monitored over 72 h by recording $^1H$ NMR spectra at different time intervals.

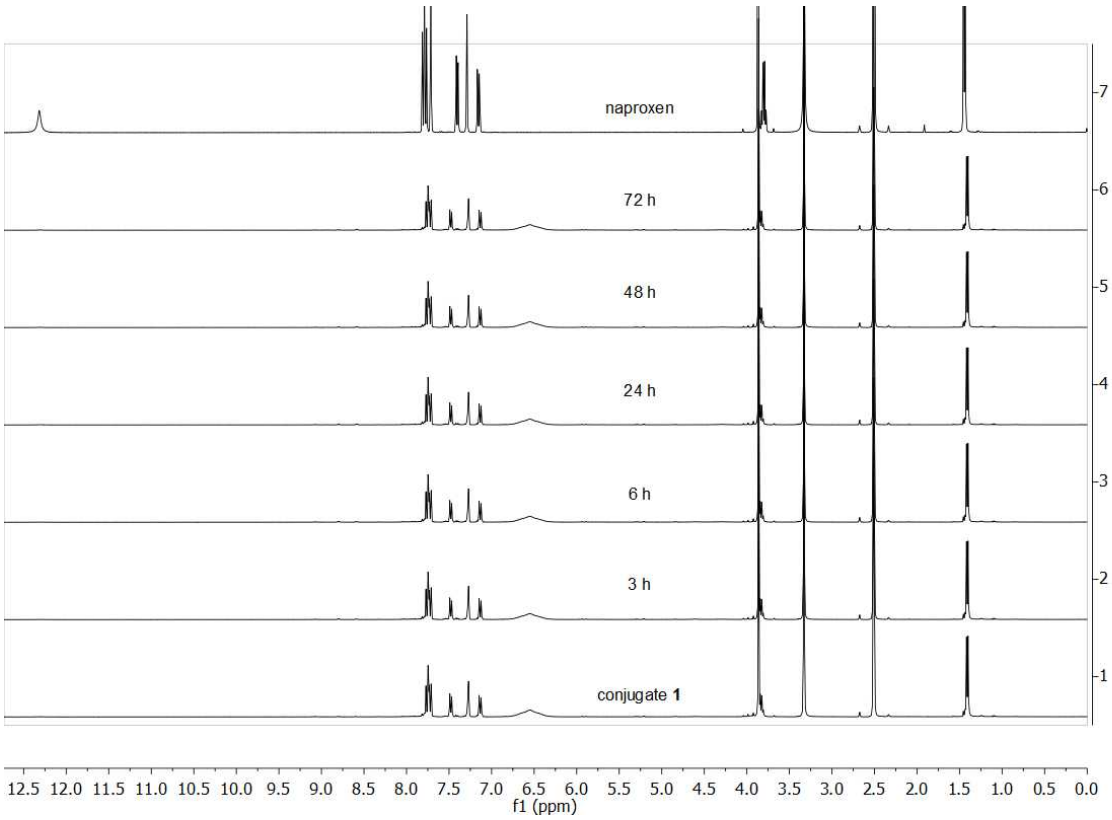


**Figure S 14.** Stability of conjugate **1** in DMSO solution; time-resolved $^{1}$H NMR spectra (400 MHz, $d_6$-DMSO).

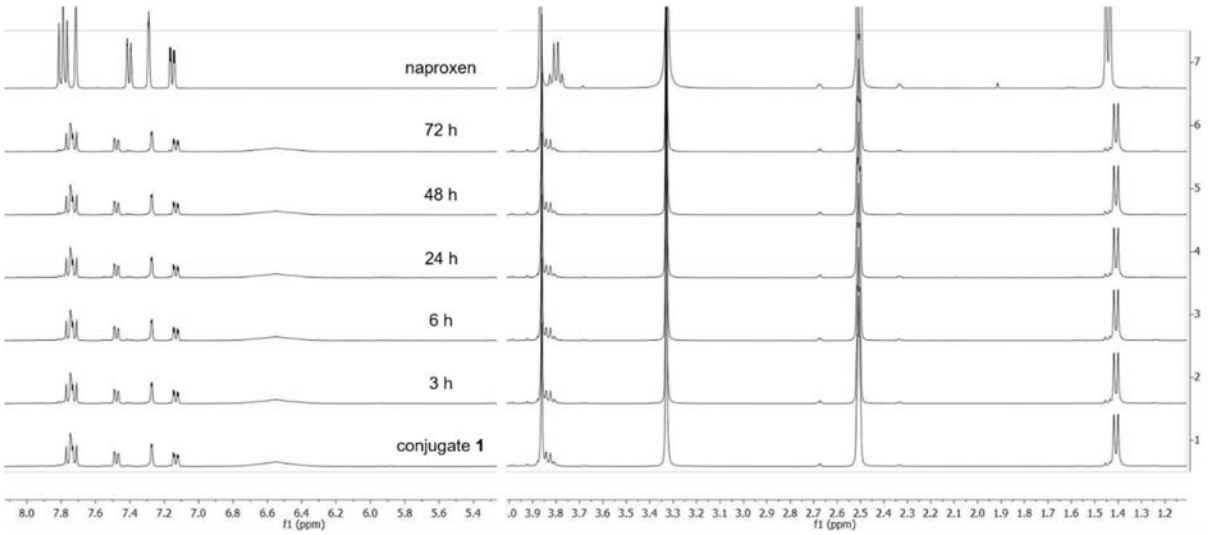


**Figure S 15.** Stability of conjugate **1** in DMSO solution; time-resolved $^{1}$H NMR spectra (400 MHz, $d_6$-DMSO); sections of the aromatic and aliphatic region.

## Recalculation of the $IC_{50}$ [μM] values

The recalculation of the $IC_{50}$ [μM] values for the immobilised compounds SBA-15|**1**, SBA-15|**2** and SBA-15|**3** from the obtained $MC_{50}$ [μg $mL^{-1}$] values was conducted as following:

**Step 1:**

- Quantification of the amount of platinum in the drug-loaded mesoporous silica nanoparticles (MSNs) achieved by energy dispersive X-ray analysis (EDX) analysis.

First, the spatial distribution of silicon and platinum was determined through mapping in order to evaluate whether the distribution of the drugs (**1**, **2** and **3**) in the corresponding drug-loaded materials (SBA-15|**1**, SBA-15|**2** and SBA-15|**3**) was homogeneous. After homogeneous distribution of the drugs was confirmed for all materials (as shown in Figure S16), the amount of platinum in the drug-loaded MSNs was quantified by:

- determination of the relative weight % of silicon and platinum at six randomly chosen points (results presented in Table S1);
- calculating the Pt/Si ratio based on the found relative weight % (0.33, 0.41 and 0.35 for SBA-15|**1**, SBA-15|**2** and SBA-15|**3**, respectively);
- calculating the entrapment efficiency by comparing the calculated Pt/Si ratio to the theoretical one (78.9 %, 98.5 % and 83.5 % for SBA-15|**1**, SBA-15|**2** and SBA-15|**3**, respectively);
- calculating the load content of platinum based on the theoretical weight % of platinum and the corresponding entrapment efficiency (8.68 wt%, 11.23 wt% and 9.10 wt% for SBA-15|**1**, SBA-15|**2** and SBA-15|**3**, respectively).

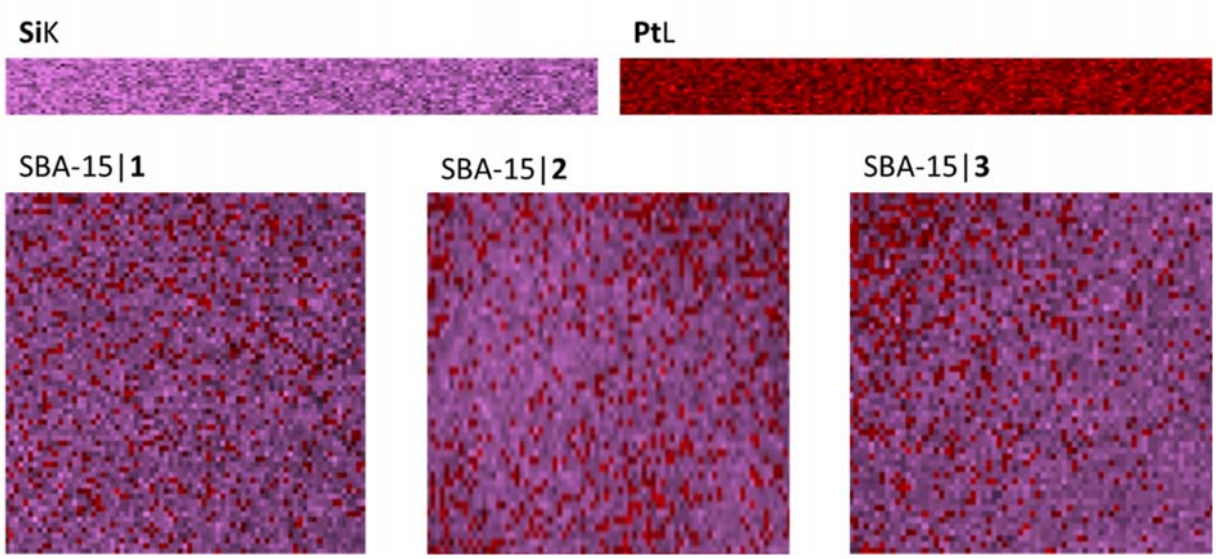


**Figure S16.** Spatial distribution of silicon and platinum in SBA-15|**1**, SBA-15|**2** and SBA-15|**3** determined through EDX mapping.

**Table S1.** Relative weight % of silicon and platinum at six points in SBA-15|**1**, SBA-15|**2** and SBA-15|**3** determined by EDX analysis.

| | SBA-15\|**1** | | SBA-15\|**2** | | SBA-15\|**3** | |
|---|---|---|---|---|---|---|
| | **Si** | **Pt** | **Si** | **Pt** | **Si** | **Pt** |
| | wt% | | | | | |
| | 74.4 | 25.6 | 73.8 | 26.2 | 77.7 | 22.3 |
| | 74.2 | 25.8 | 64.5 | 35.5 | 73.6 | 26.4 |
| | 71.7 | 28.3 | 67.6 | 32.4 | 77.8 | 22.2 |
| | 78.1 | 20.9 | 74.4 | 25.6 | 71.0 | 29.0 |
| | 77.6 | 22.4 | 77.2 | 22.8 | 67.0 | 33.0 |
| | 75.6 | 24.4 | 68.1 | 31.9 | 77.8 | 22.2 |
| **Average:** | **75.3** | **24.6** | **70.9** | **29.1** | **74.2** | **25.9** |

**Step 2:**

- Calculation of the molecular weight of the drug-loaded materials.

The molecular formula of the drug-loaded materials (Table S2) was established based on the calculated entrapment efficiency and platinum load given above. Consequently, the molecular weight of these compounds was calculated (Table S2).

**Table S2.** Molecular formula and molecular weight of SBA-15|**1**, SBA-15|**2** and SBA-15|**3.**

| Compound | Molecular formula | Molecular weight [g $mol^{-1}$] |
|---|---|---|
| SBA-15\|**1** | **1** x 21 SBA-15 | 2033.56 |
| SBA-15\|**2** | **2** x 17 SBA-15 | 1731.59 |
| SBA-15\|**3** | **3** x 20 SBA-15 | 1981.62 |

**Step 3:**

- Calculation of the percentage of drug released from the MSNs over 72 h.

The procedure followed for performing the drug release studies is described in the main text.

The percentage of drug released over 72 h was calculated based on the platinum content detected in the liquid phase by ICP-OES and the theoretical platinum content, and drug release of 73.8 %, 92.9 % and 90.5 %. was found for SBA-15|**1**, SBA-15|**2** and SBA-15|**3**, respectively.

**Step 4:**

- Recalculation of the $IC_{50}$ values from the $MC_{50}$ values.

The $IC_{50}$ values were calculated by dividing the established $MC_{50}$ values by the molecular weight of the respected compound calculated in Step 2 and, additionally, taking into account the percentage of drug released over 72 h given in Step 3.

## Drug release kinetics

The kinetics of the drug release were studied by fitting the *in vitro* drug dissolution data to four different model-dependent methods: zero-order, first-order, Higuchi and Korsmeyer Peppas models.

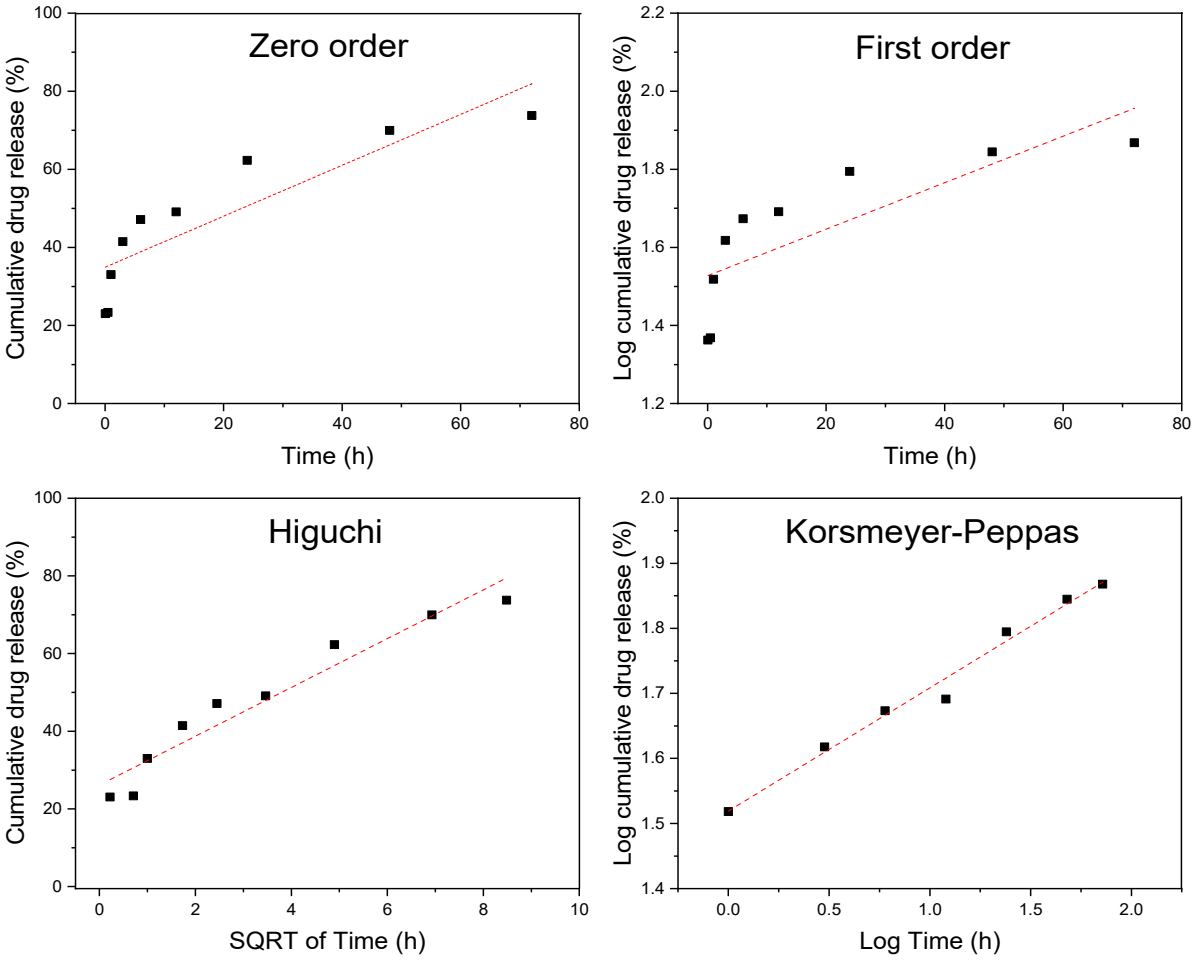


F**igure S17**. Zero order, first order, Higuchi and Korsmeyer-Peppas kinetic of the release of **1** from SBA-15⊃**1**.

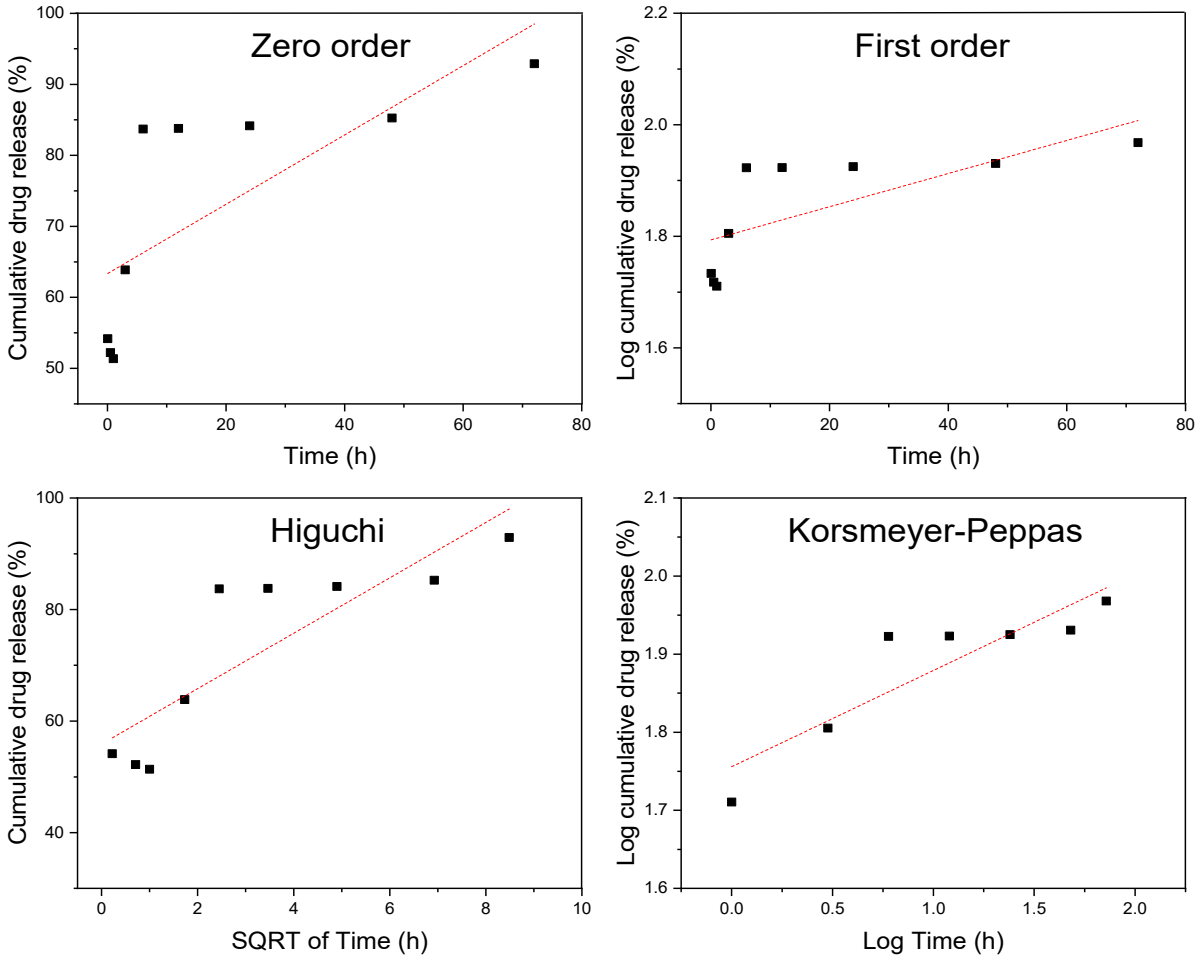


**Figure S18.** Zero order, first order, Higuchi and Korsmeyer-Peppas kinetic of the release of **2** from SBA-15|**2**.

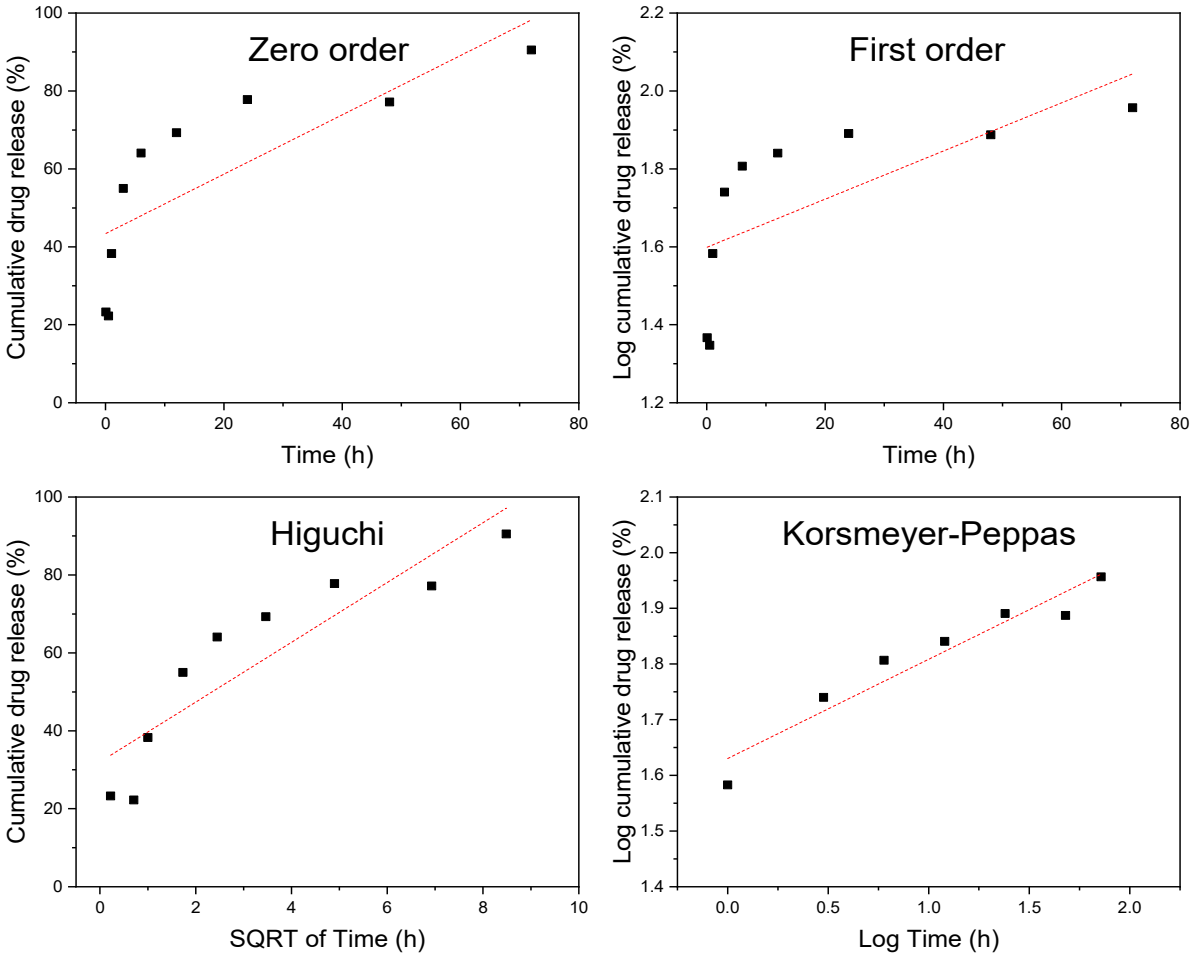


**Figure S19.** Zero order, first order, Higuchi and Korsmeyer-Peppas kinetic of the release of **3** from SBA-15|**3**.

**Table S3.** The constants and coefficient of determinations ($R^2$) for each model.

| | Zero order | | First order | | Higuchi | | Korsmeyer–Peppas | |
|---|---|---|---|---|---|---|---|---|
| | $K^0$ | $R^2$ | $Q_{inf}$ | $R^2$ | $K_h$ | $R^2$ | n | $R^2$ |
| SBA-15\|**1** | 0.653 | 0.776 | 0.014 | 0.639 | 6.282 | 0.934 | 0.189 | 0.985 |
| SBA-15\|**2** | 0.488 | 0.551 | 0.007 | 0.513 | 4.967 | 0.742 | 0.123 | 0.807 |
| SBA-15\|**3** | 0.762 | 0.618 | 0.014 | 0.474 | 7.672 | 0.815 | 0.178 | 0.927 |

## Cell viability of conjugates and corresponding MSNs

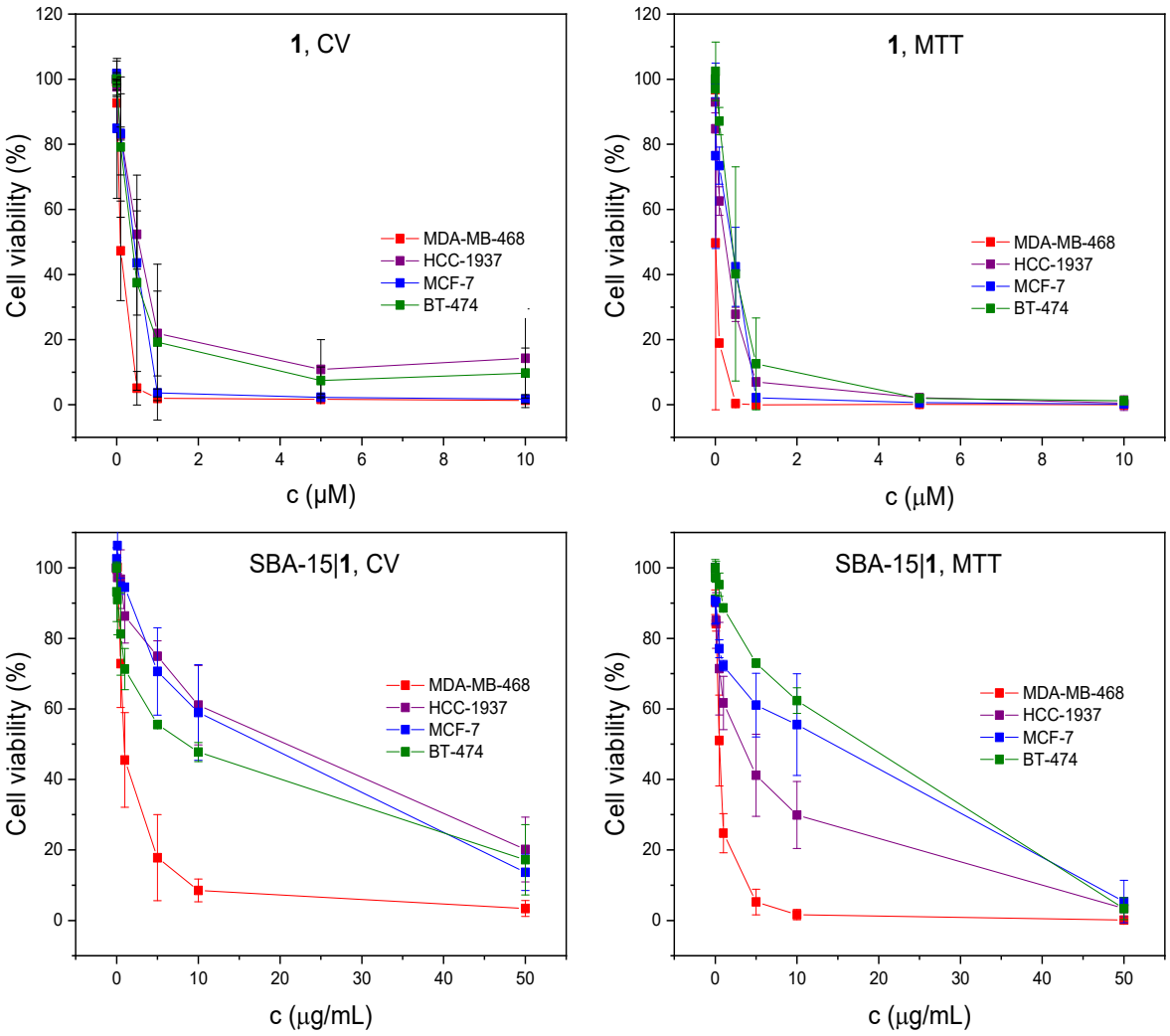


**Figure S20.** Cell viability of **1** and SBA-15|**1** determined by CV and MTT assays in four breast cancer cell lines: MDA-MB-468, HCC-1937, MCF-7 and BT-474.

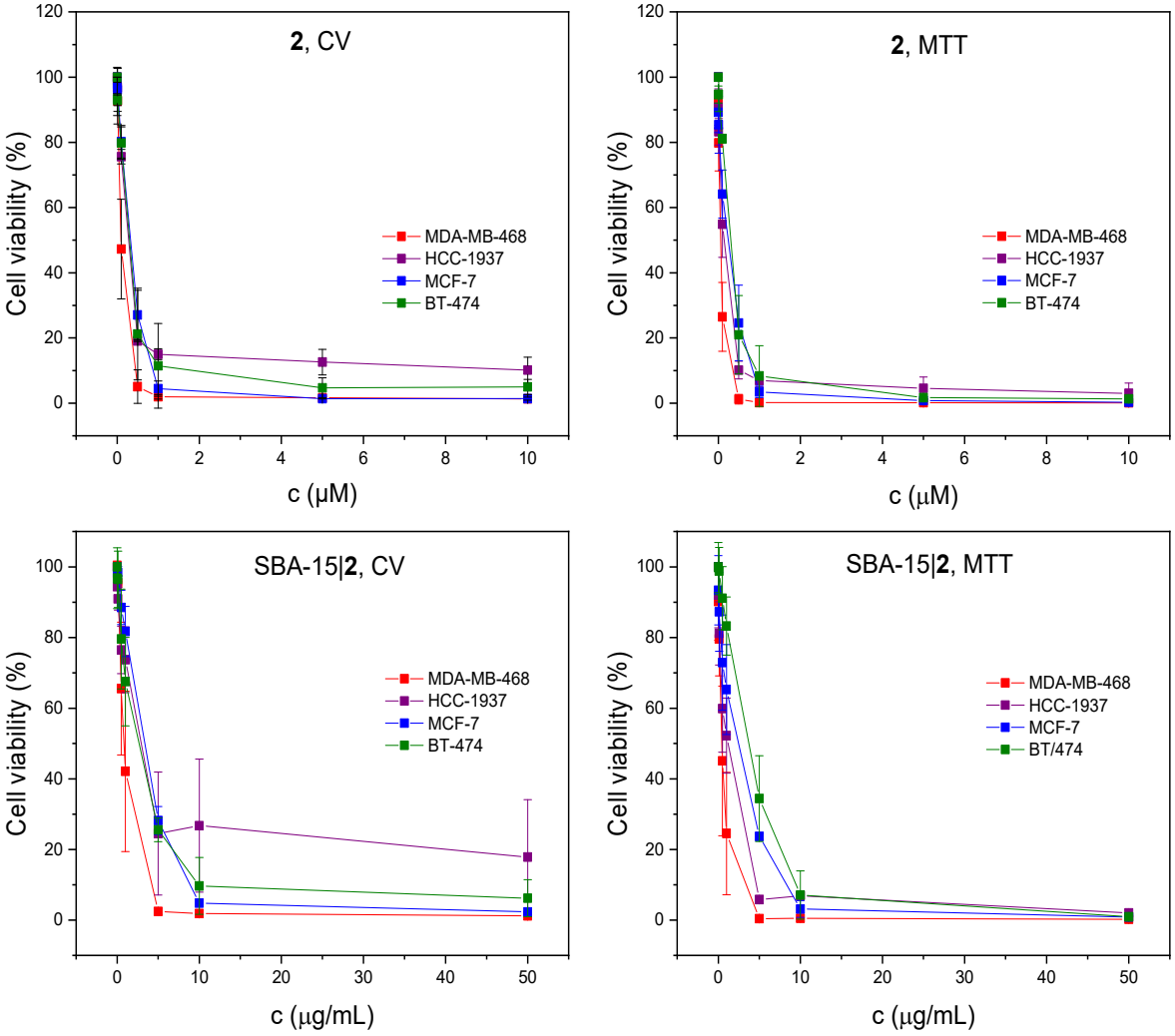


**Figure S21.** Cell viability of **2** and SBA-15|**2** determined by CV and MTT assays in four breast cancer cell lines: MDA-MB-468, HCC-1937, MCF-7 and BT-474.

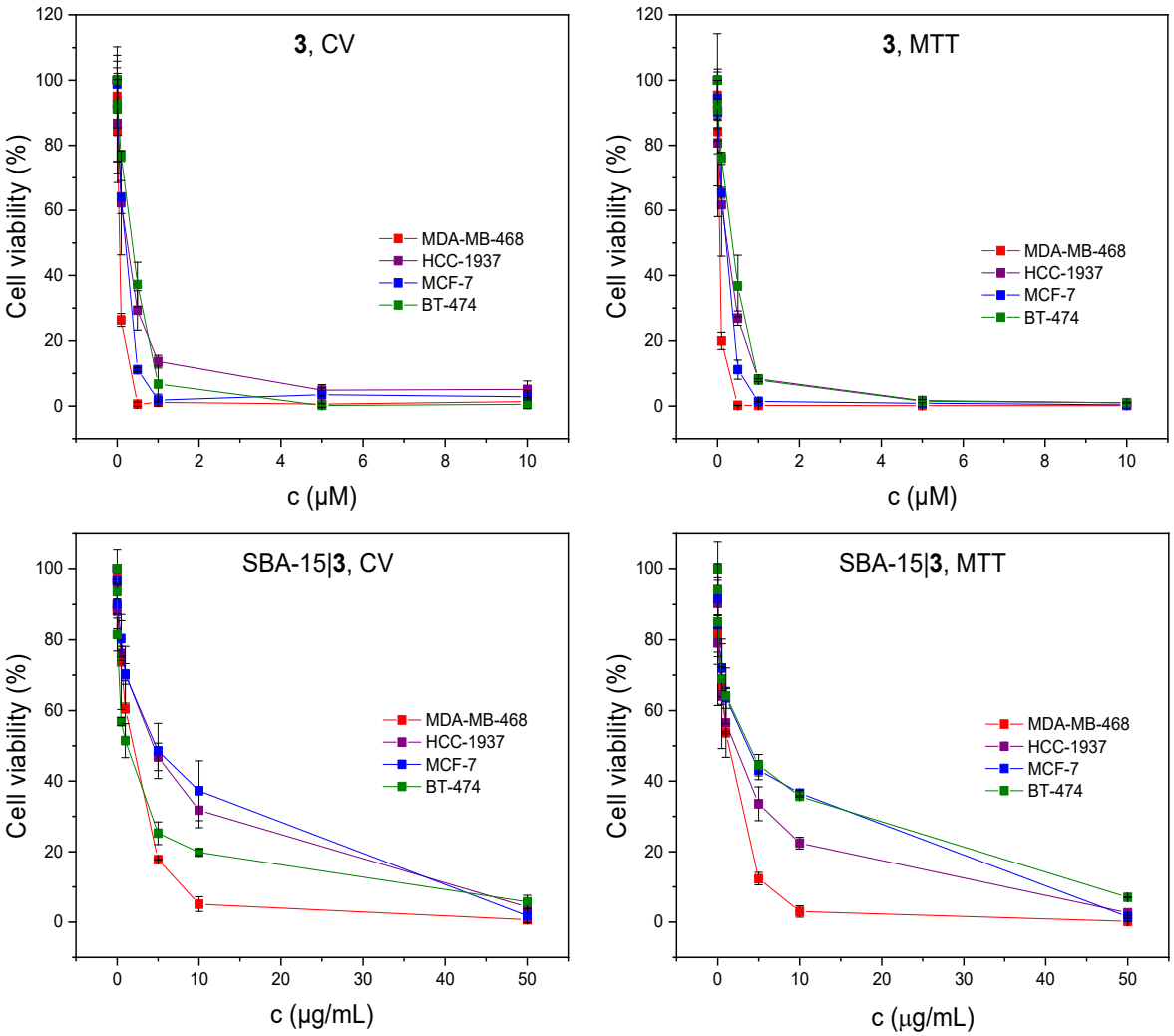


**Figure S22**. Cell viability of **3** and SBA-15|**3** determined by CV and MTT assays in four breast cancer cell lines: MDA-MB-468, HCC-1937, MCF-7 and BT-474.